

AD-A036 452

FLORIDA UNIV GAINESVILLE DEPT OF ENGINEERING SCIENCES F/G 20/9
TWO-PHASE HARTMANN FLOWS IN THE MHD GENERATOR CONFIGURATION.(U)
JAN 77 E R LINDGREN, U H KURZWEG, R E ELKINS N00014-76-C-0410

UNCLASSIFIED

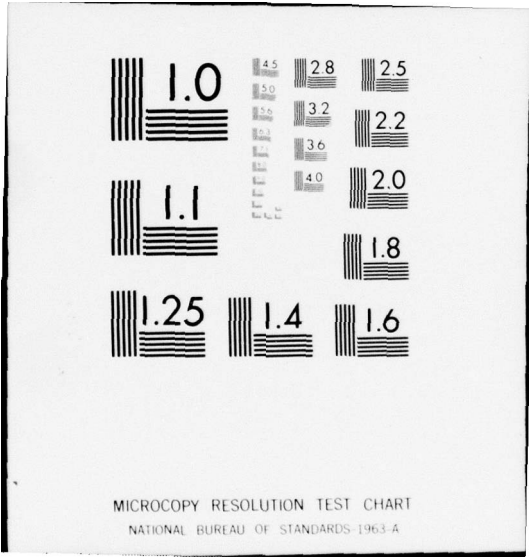
NL

1 of 1
ADA036452



END

DATE
FILMED
3 - 77



ADA 036452

12
B.S.

Annual Report
(Dec. 1975-Dec. 1976)

On

TWO PHASE HARTMANN FLOWS

IN THE

MHD GENERATOR CONFIGURATION

by

E.R. Lindgren, U.H. Kurzweg, R.E. Elkins, and T.A. Trovillion

DEPARTMENT OF ENGINEERING SCIENCES
UNIVERSITY OF FLORIDA
Gainesville, Fla. 32611

Contract N 00014-76-C-0410

NR 099-412

Office of Naval Research

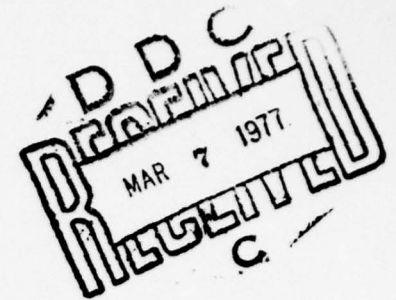
January 1977

APPROVED FOR PUBLIC RELEASE
DISTRIBUTION UNLIMITED

DDC
MAR 7 1977
C

[Handwritten signatures and scribbles]

**Annual Report
(Dec. 1975-Dec. 1976)**



On

**TWO PHASE HARTMANN FLOWS
IN THE
MHD GENERATOR CONFIGURATION**

by

E.R. Lindgren, U.H. Kurzweg, R.E. Elkins, and T.A. Trovillion

**DEPARTMENT OF ENGINEERING SCIENCES
UNIVERSITY OF FLORIDA
Gainesville, Fla. 32611**

Contract N 00014-76-C-0410

NR 099-412

Office of Naval Research

January 1977

ABSTRACT

Two-phase Hartmann flows in an MHD generator duct of rectangular cross-section are examined and numerical values for the velocity fields and induced current streamlines for fluids of spatially-dependent electrical conductivity are determined as a function of load factor, Hartmann number and channel aspect ratio. This study is of considerable practical interest in connection with some experimental work in progress at Argonne Laboratories on two phase liquid metal-gas MHD generators and the results presented herein may enhance the understanding of the operating characteristics of such devices. The problems considered include: 1) one-dimensional Hartmann flow between two parallel plates at high Hartmann number when the fluid electrical conductivity decreases with increasing distance from the walls, 2) two-dimensional Hartmann flow in rectangular channels of finite aspect ratio having two insulating walls and two thin walls of finite conductivity representing the electrodes and, 3) compressible one-dimensional isothermal MHD flow with zero-slip between its liquid and gas components. Results indicate that conductivity gradients can produce inflected velocity profiles which may be hydrodynamically unstable, that for larger load factors the shunt current in the Hartmann boundary layers become considerable and that two-phase MHD flows of moderate void fractions have sound speeds considerably lower than in its components. Turbulent effects are not considered in these studies since turbulent fluctuations are expected to be suppressed for the high Hartmann number flows of interest in two-phase MHD generators.

ACCESSION YR	
NTIS	White Section <input checked="" type="checkbox"/>
DISC	Brit Section <input type="checkbox"/>
UNANNOUNCED	<input type="checkbox"/>
JUSTIFICATION	
BY DISTRIBUTION/AVAILABILITY CODES	
Dist.	MAIL and/or SPECIAL
A	

TABLE OF CONTENTS

	Page
Abstract	i
List of Symbols	iii
I. Introduction	1
II. One-Dimensional Hartmann Flow with Variable Electrical Conductivity	3
III. Two-Dimensional Hartmann Flows in Channels of Rectangular Cross-Section	10
IV. Two-Phase, Zero-Slip Model for Compressible MHD Flow	20
V. Concluding Remarks	26
References	28
Report Documentation Page, Form DD 1473	

LIST OF SYMBOLS

x	co-ordinate perpendicular to the flow direction and the applied magnetic field
y(or Y)	co-ordinate parallel to the applied magnetic field
z	co-ordinate in flow direction
t	time
a	channel half-width in y direction
b	channel half-width in x direction
B_0	applied magnetic intensity
E	induced electric field in x direction
L	channel length in flow direction
R	external electrical resistance
K	load factor (= ratio of external to total electrical resistance)
H	half-height of channel in y direction for one-dimensional problem
c	sound velocity in homogeneous two-phase mixtures
r	channel aspect ratio (= b/a)
P	total pressure (hydrodynamic and magnetic)
$\frac{\partial p}{\partial z}$	pressure gradient in flow direction
W	velocity in flow direction
B	induced magnetic intensity in flow direction
K_w	ratio of electrode resistance to fluid plus electrode resistance
α	void fraction (= ratio of gas to total volume)
μ	coefficient of viscosity
σ	electrical conductivity
μ_e	magnetic permeability
η	magnetic viscosity (= $1/\mu_e \sigma$)
ρ	density
γ	specific heat ratio of gas component
M	Hartmann number (= $aB_0 \sqrt{\sigma_0/\mu_0}$)
N	Interaction parameter (= $\sigma_0 B_0^2 L/\rho W$)

Subscripts

o	value at channel walls
g	gas component of two-phase flow
l	liquid component of two-phase flow

I. INTRODUCTION

An analytical study on two-phase Hartmann flows in the MHD generator configuration has been in progress here at the University of Florida since December 1975. The objective of this ONR sponsored program has been to better understand the behaviour of electrically conducting flows with spatially dependent electrical conductivity in the presence of externally applied magnetic fields and in particular to aid in the understanding of some of the experimental observations which have been and are being obtained in a major experimental research program at Argonne Laboratories on liquid metal-gas MHD power generation[1, 2]. The hydromagnetic flow behaviour in such two-phase devices is of special interest to the Navy as these generators, if they can be made to function in scaled-up versions, have good efficiencies and high power densities which would make them ideally suited for on-board applications. At the present time an effort is underway at Argonne Laboratories to construct a two-phase, sodium-argon MHD generator with a net 30 MW power output[1]. It is part of our effort at the University of Florida to gain a better understanding of the properties of the MHD flows encountered in such generators and possibly to aid in the surmounting of expected difficulties introduced by upscaling, end effects and liquid-gas separation within the generator channel. We have made an effort to initiate and maintain communications between the various research groups working in liquid metal-gas MHD power generation. Discussions to date have been held, among others, with M. Petrick's Group at Argonne Laboratories and with H. Branover of Ben-Gurion University.

The present report gives a summary of results obtained by us here at the University of Florida during the first year of the contract period.

The personnel involved in the combined analytical-numerical research effort have been Drs. E. R. Lindgren and U. H. Kurzweg as co-principal investigators , together with R. E. Elkins as a full-time post-doctoral investigator and T. A. Trovillion as a PhD candidate. The initial phase of our study included a careful examination of the relevant literature in the field and a formulation of an appropriate set of equations governing two-phase magnetohydrodynamic flows. This was followed by major analytical efforts in the areas of: 1) One-dimensional Hartmann flow for fluids of variable electrical conductivity, 2) Two-dimensional Hartmann flow in channels of rectangular cross-section and 3) One-dimensional compressible MHD flow under zero-slip conditions. Details of our results in these areas are presented below.

II. ONE-DIMENSIONAL HARTMANN FLOW WITH VARIABLE ELECTRICAL CONDUCTIVITY

Our initial studies involved the determination of velocity and current distributions in one-dimensional Hartmann flow between two parallel plates when the fluid electrical conductivity and viscosity was a function of the normal distance from the bounding walls and a constant external magnetic field was applied. This represents a first approximation to homogeneous, laminar, two-phase flow in an MHD channel of large aspect ratio when bubble motion relative to that of the liquid is neglected. The appropriate differential equation for such a laminar, one-dimensional flow in this geometry can be derived from the standard continuum MHD equations as given for example by Hughes and Young [3] and reads

$$0 = -\frac{\partial p}{\partial z} + \frac{\partial}{\partial y} \left[\mu(y) \frac{\partial W}{\partial y} \right] - \sigma(y) B_0^2 \left[W + \frac{E}{B_0} \right], \quad (1)$$

where $\mu(y)$ is the viscosity and $\sigma(y)$ the electrical conductivity both of which are taken as functions of the normal distance from the walls. Here z is the flow direction coordinate, $W(y)$ the axial velocity, B_0 the constant applied magnetic intensity in the y direction, E the electric field in the current flow direction x and $\partial p/\partial z$ the constant pressure gradient. As we were attempting to approximate the experimental conditions encountered in the Argonne Group's studies [2], the electrical conductivity was assumed to have the void related y dependence given by the empirical formula

$$\sigma = \sigma_0 [0.97083 - 1.04679 \alpha - 2.22367 \alpha^2 + 3.52146 \alpha^3 - 1.11742 \alpha^4] \quad (2)$$

with a parabolic void distribution

$$\alpha = 0.7 - 0.5(y/H)^2 = \text{Gas Volume/Total Volume} \quad (3)$$

corresponding to that found at station 4 in their non-tapered channel experiments. Here $y=\pm H$ are the locations of the bounding walls. Note again that in this model the two-phase liquid metal-gas mixture is being treated as a homogeneous fluid with variable

conductivity properties. Although such an approach is certainly not exact, it nevertheless can be expected to shed valuable new light on the problem. Also it should be noted that we are applying Eq.(2) to yield a spatial variation for σ , while the original Argonne Laboratory results [2] gave this conductivity behaviour as an averaged value across the channel in the absence of a magnetic field. Because of this difference, we may treat Eq.(2) as one among many experimental conduction formulas showing a monotonically decreasing electrical conductivity with increasing distance from the bounding walls of the channel. The viscosity coefficient in our calculations is taken as constant. This simplifying assumption is reasonable as viscous effects can be expected to be confined to a very narrow region near the walls for the high Hartmann number cases of interest. In such a thin Hartmann layer the viscosity coefficient can be treated essentially as constant although it may vary considerably in the core of the flow. The boundary conditions for the problem are the no slip velocity condition $W(\pm H)=0$ and the integral requirement

$$E = \frac{RL}{2b} \int_{-H}^{+H} \sigma(y) (WB_0 + E) dy, \quad (4)$$

where R is the external applied resistance, L is the channel length in the flow direction and 2b is the distance between electrodes in the x direction.

Equation (1), subjected to the stated boundary conditions, was solved by both an analogue and digital numerical approach since analytic solutions were not found to be possible for the conductivity distribution given by Eqs. (2) and (3) except within the core of the flow. The analogue solutions were obtained for Hartmann numbers $M=B_0H\sqrt{\sigma_0/\mu}$ up to 10 but the solution became unstable for still larger values. This difficulty is due to the rapid change in magnitude of the velocity profile in the wall near region for larger M and led us to abandon the analogue calculations in

favor of the finite difference digital approach. The digital calculations were carried out by dividing the channel half-width $0 < y < H$ into ten equally spaced subintervals within the Hartmann boundary layer located approximately in $H > y > H[1 - (1/M)]$ and ten equally spaced subintervals between the boundary layer edge and the channel axis at $y=0$. In this manner a simple matrix inversion yielded solutions for $W(y)$ for any desired Hartmann number and calculations for both constant conductivity and the variable distribution given by Eqs. (2) and (3) were made for Hartmann numbers as high as $M=1000$ without encountering convergence difficulties. Typical results for the velocity variation in the variable conductivity case are shown in Fig. 1 for $M=50$. Note the thin Hartmann layer near $y=H$ and the general inflected profile in the core of the flow. This inflection is due to the rapid decrease in electrical conductivity with increasing distance from the wall as predicted by Eq.(2) and (3) and is not present in the classical Hartmann solution where the conductivity is constant. Such inflected velocity profiles are known to be unstable from hydrodynamic stability considerations and may therefore produce a breakdown and subsequent cross-flow mixing under variable conductivity conditions. The functional form of the velocity distribution is seen to remain unchanged with varying external load, a fact well known for constant conductivity calculations. Note also that the velocity variation in the core goes approximately as the inverse of the electrical conductivity as can also be directly surmised from Eq.(1), upon neglecting the viscous term, which has significant values only in the wall near region. That is, outside the Hartmann boundary layer the velocity profile is given by an algebraic expression involving σ , B_o , E and the pressure gradient and the current density there is approximately constant. Some plots of these analytically determined velocity profiles in the core

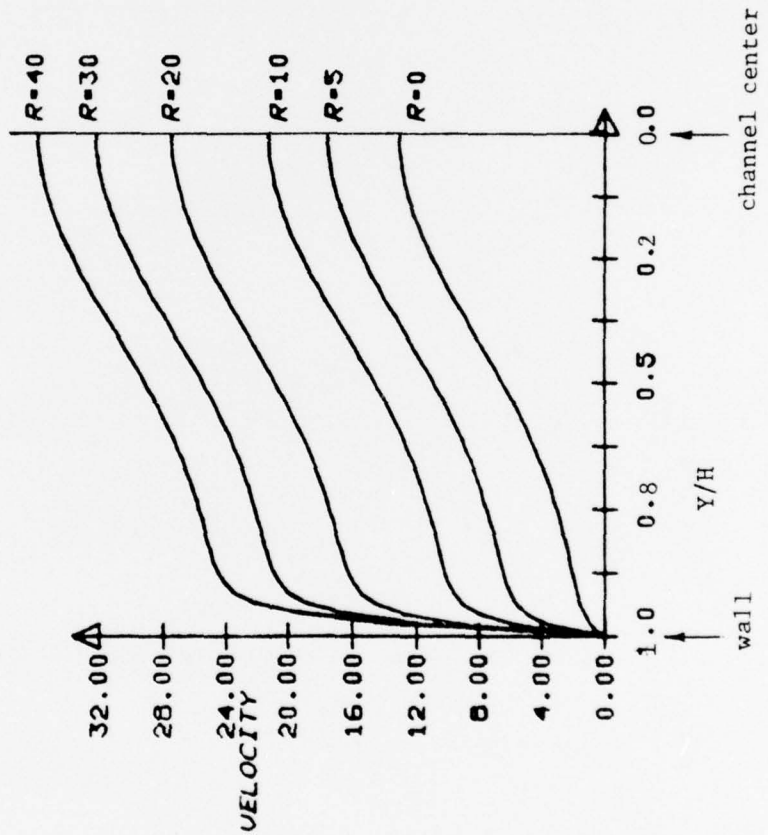
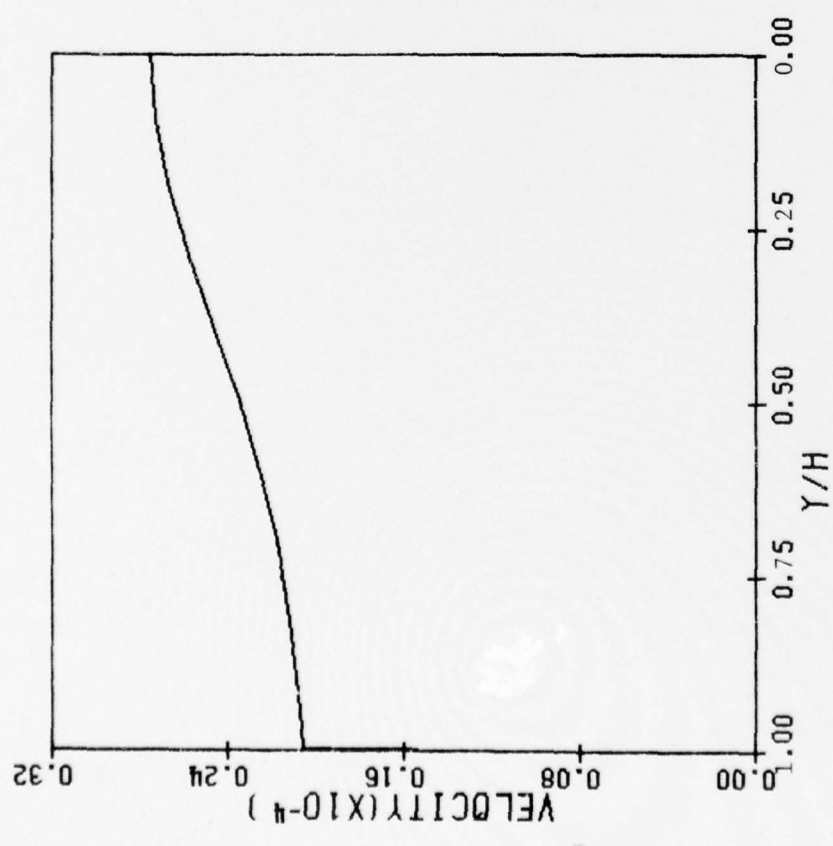
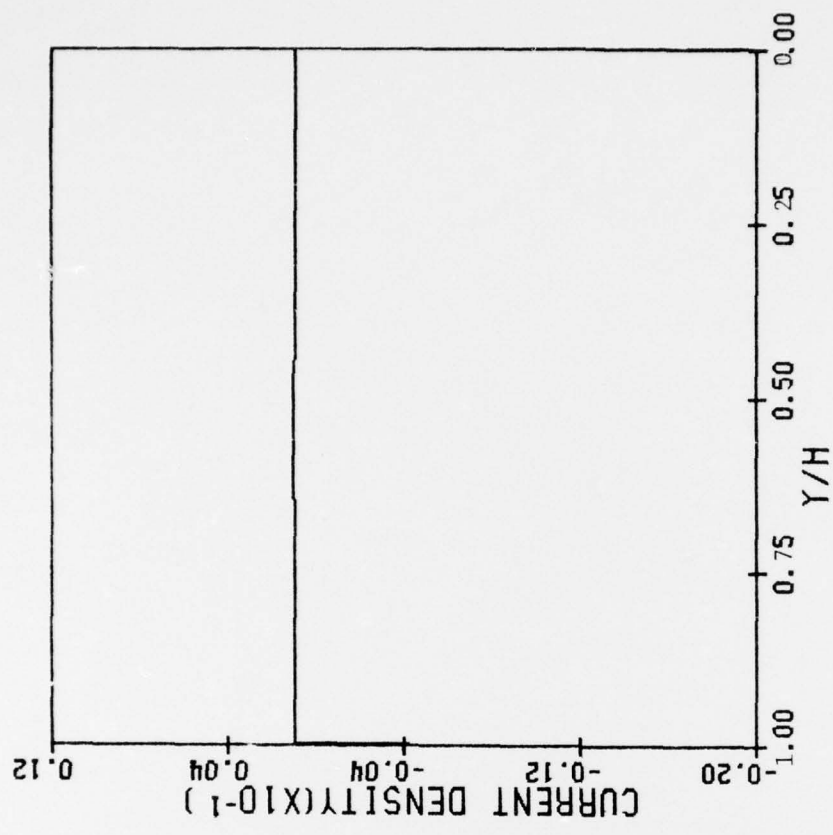


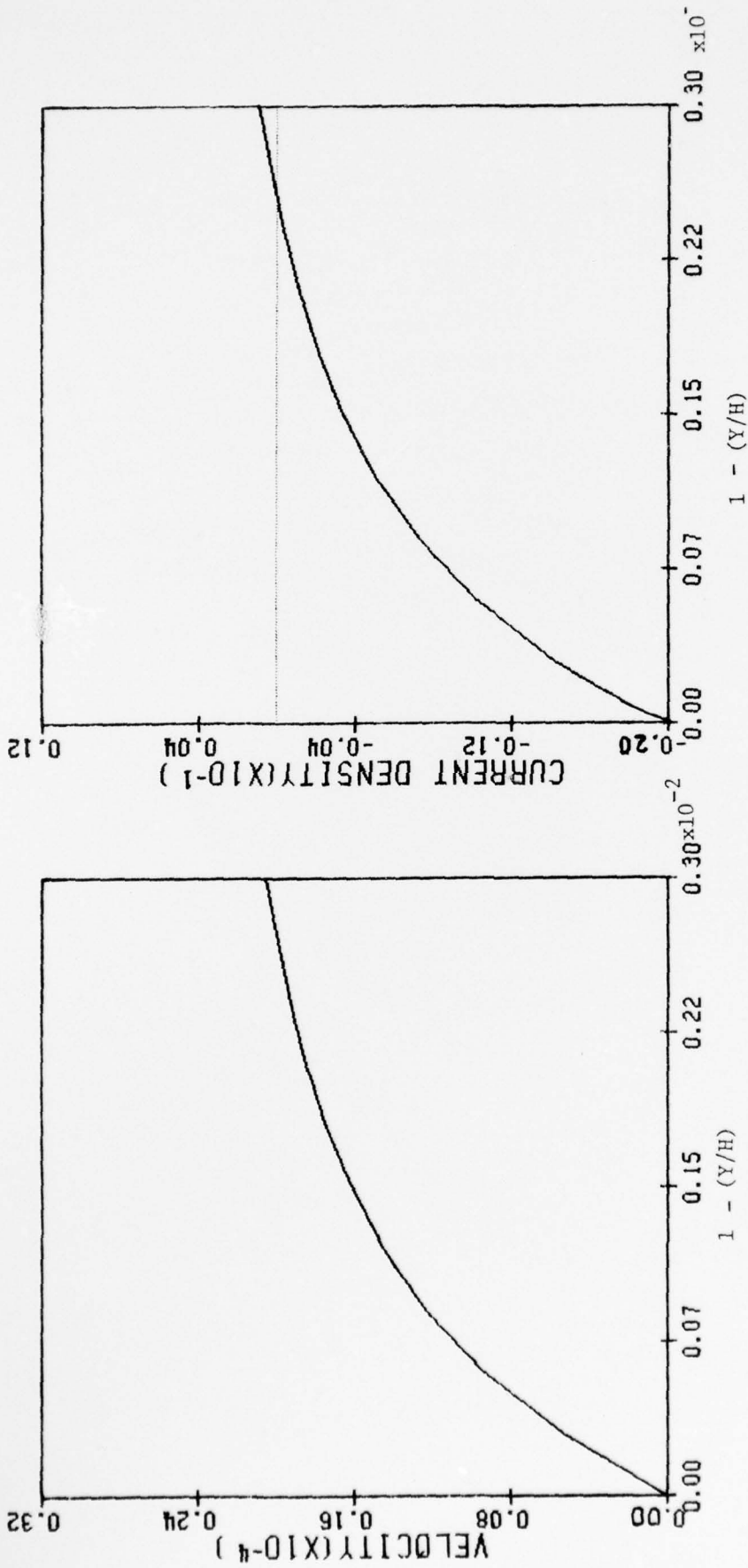
Fig. 1: One-Dimensional Hartmann Flow in a Fluid of Variable Electrical Conductivity for Different External Resistances. The Conductivity obeys Eqs. (2) and (3) and decreases toward the Channel Center. Hartmann Number $M=50$.



VELOCITY AND CURRENT PROFILES

M=1000 K=20/21

Fig. 2: Velocity and Current Profiles for One-Dimensional Hartmann Flow with Variable Electrical Conductivity. Hartmann Number M=1000, Load Factor K=20/21 and Conductivity Variation taken from Eqs. (2) and (3).



BOUNDARY LAYER PROFILES

M=1000 K=20/21

Fig. 3: Details of the Velocity and Current Profiles within the Hartmann Layer for M=1000. The Non-Conducting Wall is at y=H.

have been generated for the different void distributions given in Ref.[2] at stations 1 through 4. The velocity profiles all show a characteristic peak at the channel center where the void fraction is largest.

In figure 2 we show the velocity and electric current density in our one-dimensional channel flow for a Hartmann number of $M=1000$ and a load factor $K=R/R_{\text{total}}=20/21$. Again one notes the inflected velocity profile and the extremely thin boundary layer. The current density in the core of the flow is essentially constant. An expanded version of this same solution for the Hartmann boundary layer is found in Fig. 3 and shows the back flow current in a layer of thickness $\Delta y = 0.0025H$. We estimate that the typical Hartmann number in the Argonne liquid metal-gas MHD generator[2] is $M=400$, so that the viscous effects will be confined almost entirely to a very thin layer next to the insulating wall. We have not carried out calculations for other variable electrical conductivity profiles but can easily do so with the existing computer program. CPU time for the velocity determination for a given conductivity profile amounts to less than one second and does not increase appreciably with increasing M .

An analytical study has also been completed for these one dimensional Hartmann flows for the case of a discrete jump in electrical conductivity and viscosity coefficient at a given y between constant but differing values on the two sides of the interface. Here one finds a hyperbolic tangent type variation in the velocity $W(y)$ across the interface with the transition thickness proportional to the reciprocal of the Hartmann number. A current layer will generally exist at such a discontinuity in fluid properties.

III. TWO-DIMENSIONAL HARTMANN FLOWS IN CHANNELS OF RECTANGULAR CROSS-SECTIONS

Using the same homogeneous two-phase approximation as for the one-dimensional Hartmann flow case, we next considered laminar Hartmann flows in channels of rectangular cross-section with finite aspect ratio. Series solutions for such flows in the constant conductivity limit have been obtained by many investigators including Shercliff [4], Uflyand [5], Chang and Lundgren [6] and others. However these calculations are generally not applicable for the wall conductivities encountered in MHD generator configurations nor are the series solutions obtained well suited for numerical evaluation at high Hartmann numbers. Accordingly, instead of using the series solution method which is unlikely to work for variable conductivity conditions anyway, we went directly to a digital solution approach using a two dimensional version of a variable grid spacing such that the number of points within the boundary layers of the channel walls equal approximately those within the core of the flow. The governing momentum and magnetic induction equations governing such variable property Hartmann flows were derived and in Cartesian coordinates assume the form

$$-\frac{\partial P}{\partial z} + \frac{B_0}{\mu_e} \left(\frac{\partial B}{\partial y} \right) + \frac{\partial}{\partial x} \left(\mu \frac{\partial W}{\partial x} \right) + \frac{\partial}{\partial y} \left(\mu \frac{\partial W}{\partial y} \right) = 0 \quad (5)$$

$$B_0 \frac{\partial W}{\partial y} + \frac{\partial}{\partial x} \left(\eta \frac{\partial B}{\partial x} \right) + \frac{\partial}{\partial y} \left(\eta \frac{\partial B}{\partial y} \right) = 0 \quad , \quad (6)$$

where B_0 is the constant external magnetic field applied in the y direction, $W(x,y)$ the sought after axial velocity distribution and B the induced field in the z direction. Here P represents the total pressure and $\eta=1/\mu_e \sigma$ is the magnetic viscosity related to the magnetic permeability and electrical conductivity. We note that Eqs. (5) and (6) reduce respectively to the classical

MHD momentum and induction equations[3] in the limit of constant μ and η . The important non-dimensional parameters in the problem are the aspect ratio $r=b/a$ of the channel, where $2b$ is the distance between thin finite conductivity electrodes at $x=\pm b$ and $2a$ the distance between the two insulating sides of the channel at $y=\pm a$, and the Hartmann number here defined at $M=aB_0\sqrt{\sigma_0/\mu_0}$, where μ_0 and σ_0 are the fluid viscosity and electrical conductivity at the wall, respectively. The boundary conditions appropriate to an MHD generator channel and those used in our calculations were that W vanishes on the channel walls, that $B=\text{Const.}$ at the insulating walls and that both the tangential component of the electric field and the normal component of the magnetic intensity be continuous at the electrodes. For the finite thickness and finite electrical conductivity electrodes under consideration this leads to a mixed boundary condition at the electrodes identical to that used by Chang and Lundgren[6]. An important parameter entering the boundary conditions at the electrodes is the non-dimensional electrode resistivity, $K_W=\text{resistivity of electrode/resistivity of fluid plus electrode}$.

Numerical calculations using a variable grid spacing based upon a boundary layer thickness of a/M at the insulating surfaces and one of $a/M^{1/2}$ at the electrodes was carried out using the extended Peaceman-Rachford alternate direction implicit method[7]. The method involves a relaxation scheme in which a time derivative is introduced into the equations and the solutions relaxed until all time dependence vanishes. The advantage of this method is that all iterations are solved implicitly, considering all nodes simultaneously. This gives numerical stability to the calculations and the necessary matrix inversion is reduced to inverting a tridiagonal system.

Because of the symmetries inherent in the problem our calculations were confined to only the first quadrant of the rectangular cross-section. The velocity and magnetic intensity was evaluated at 400 mesh points within this quadrant and typically involved six seconds of computer time at a Hartmann number of 20. Typically 35 to 50 iterations were required for convergence.

Our first calculations were done for the constant electrical conductivity and viscosity case at an aspect ratio $r=b/a=2$, a Hartmann number 20, zero load factor and electrodes of infinite conductivity ($K_w=0$). Results of the calculation are shown in Figures 4 and 5. The first of these shows contours of constant velocity in increments of one-eighth the maximum velocity at the channel center. Note the relatively thick boundary layer at the electrodes compared to the narrow Hartmann layer at the insulating walls which are perpendicular to the applied magnetic field. The induced current lines (which are proportional to B) are seen to lie essentially parallel to the non-conducting walls with no appreciable return current in the Hartmann layer. This fact stems from the zero external load considered in this particular calculation. Large return currents near the insulating walls were found for large load factors as demonstrated in Figs. 6 and 7. Note in Fig. 7 that all current lines remain in the liquid as the electrodes are non-conducting ($K_w=1$). To our knowledge these calculations represent the first finite difference solutions for the Hartmann generator geometry and should be extendable without major problems to other aspect ratios and larger Hartmann numbers. As in the one dimensional case, the current density within the core of the flow is essentially constant.

Some calculations were also done for a variable conductivity fluid of assumed constant viscosity. For a choice of conductivity we considered

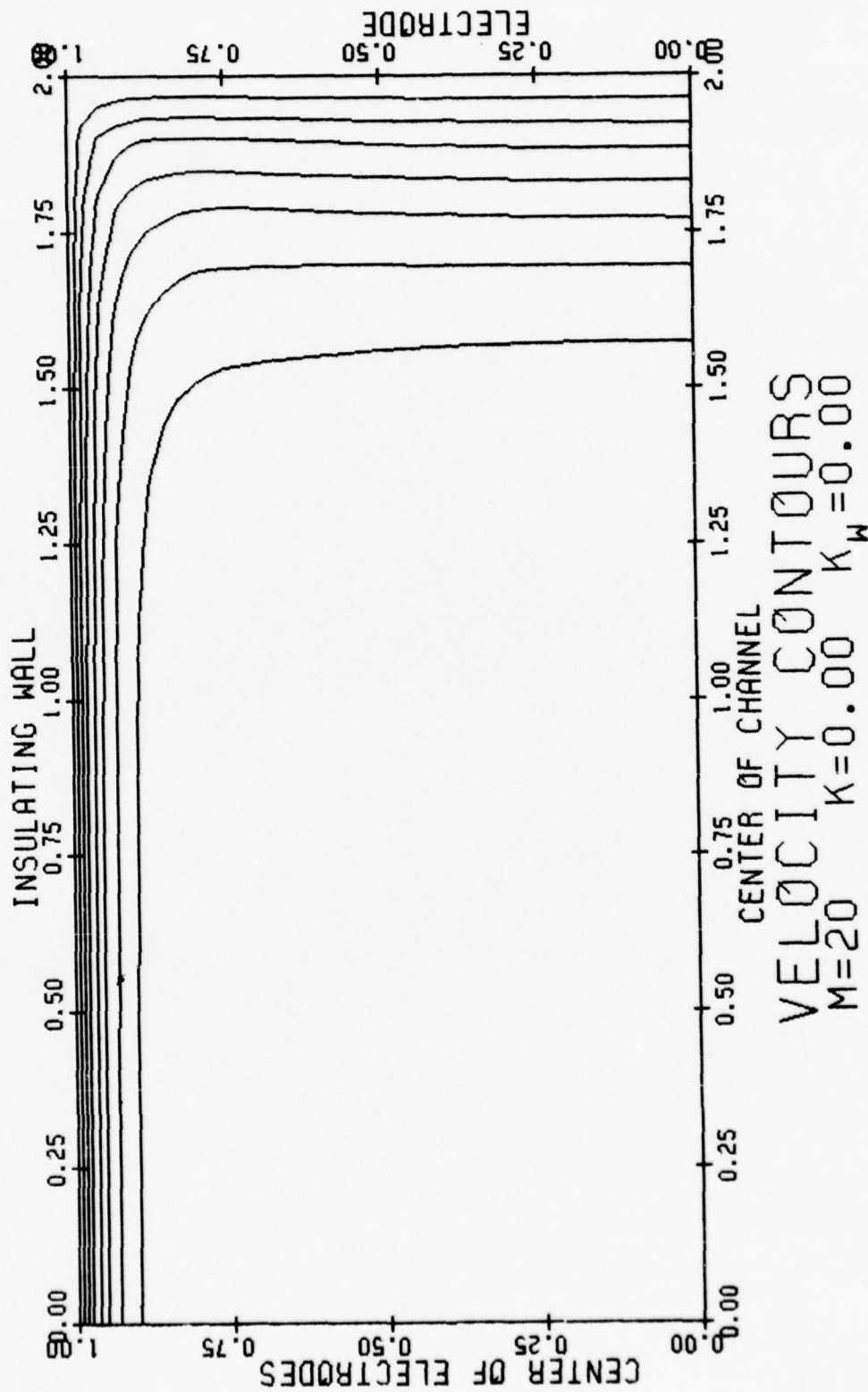


Fig. 4: Velocity Contours for Two-Dimensional Hartmann Flow in the MHD Generator Configuration. Constant Electrical Conductivity and Zero External Load. Aspect Ratio $r=b/a=2$. Hartmann Number $M=20$.

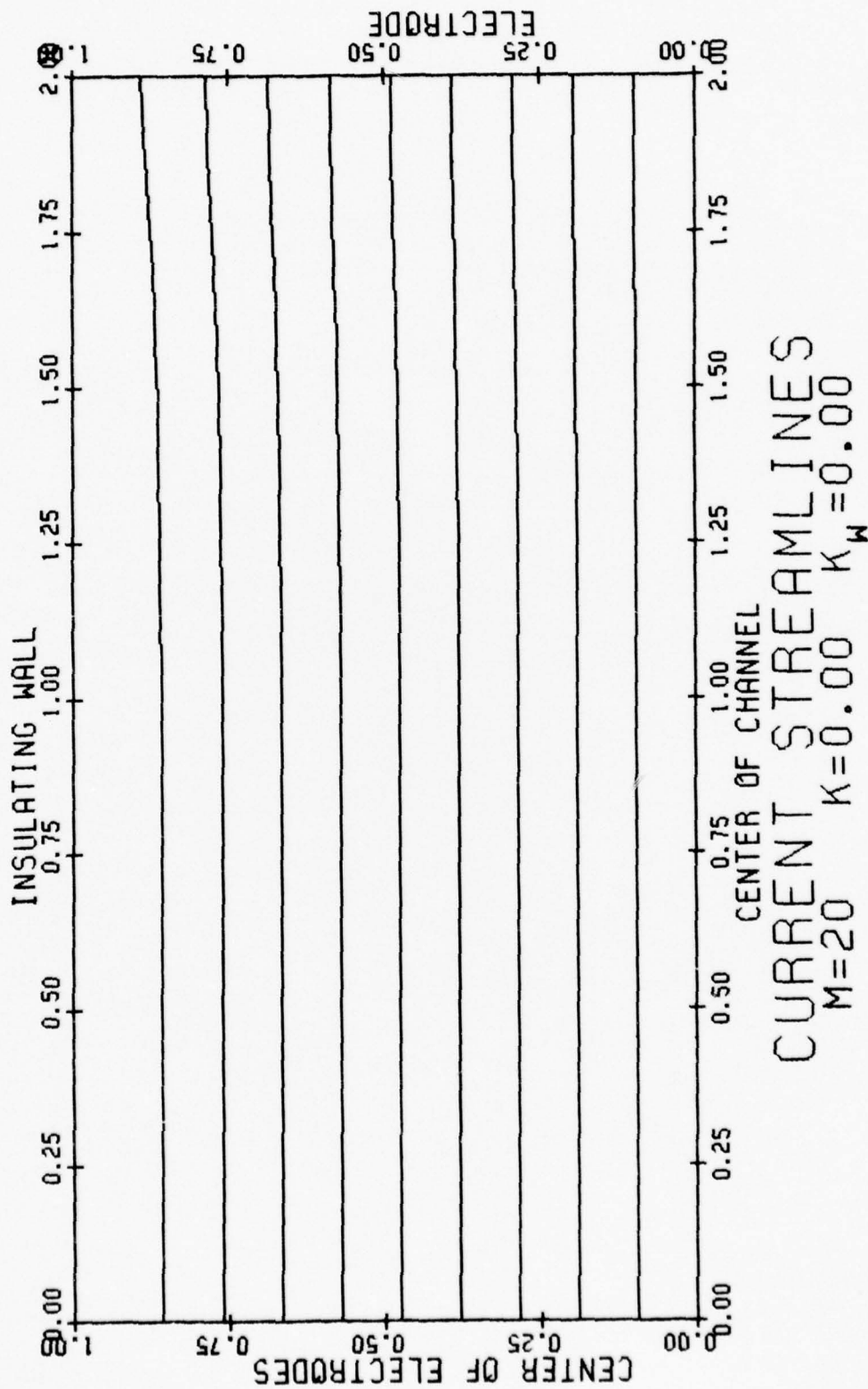


Fig. 5: Current Streamlines for Hartmann Flow in the MHD Generator Configuration. Note the Absence of Return Currents in the Hartmann Boundary Layer for the Zero Load Factor Case Considered.

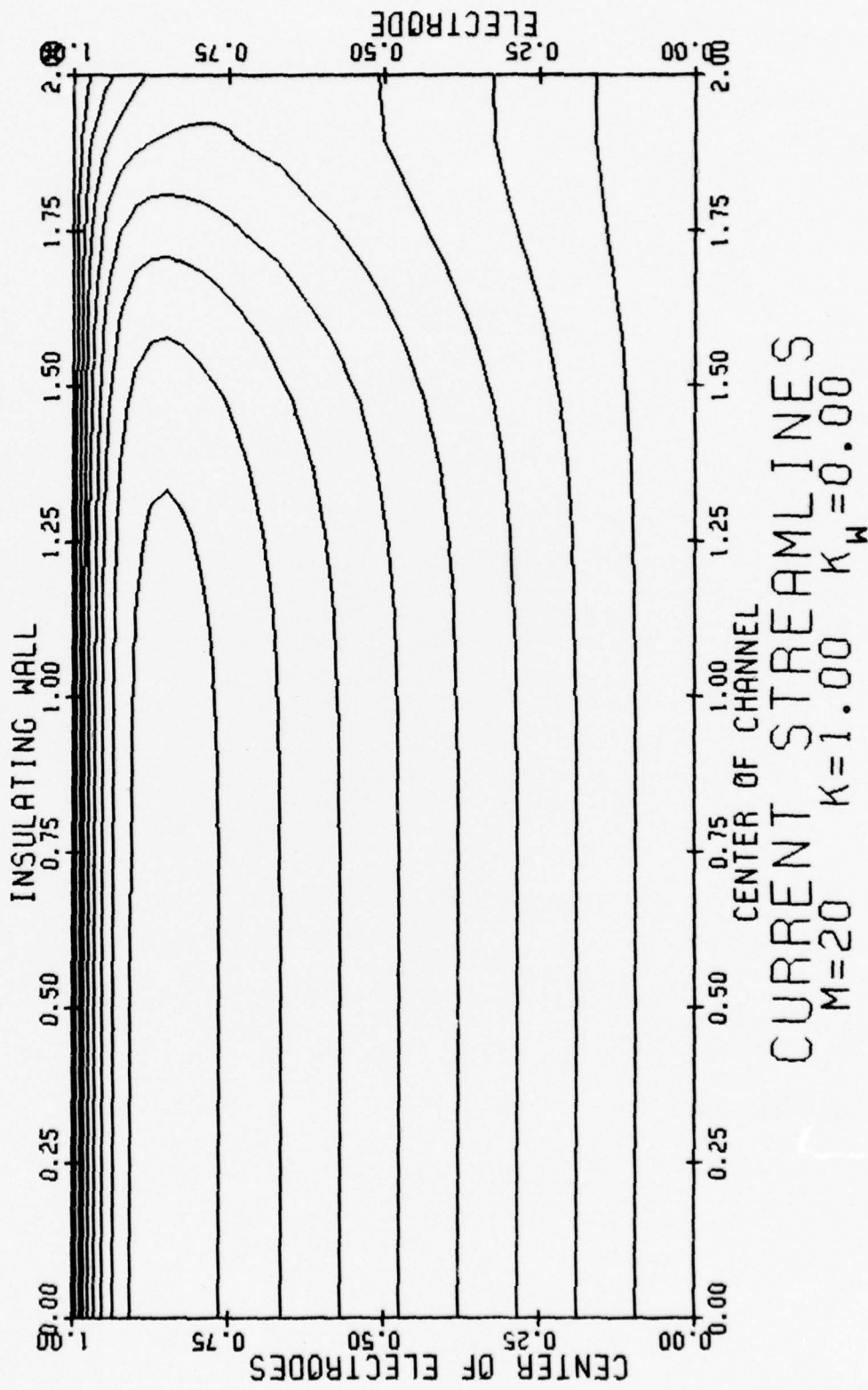


Fig. 6: Current Streamlines for Hartmann Flow in the MHD Generator Configuration with Infinite External Load ($K=1.0$) and Ideally-Conducting Electrodes ($K_W=0$).

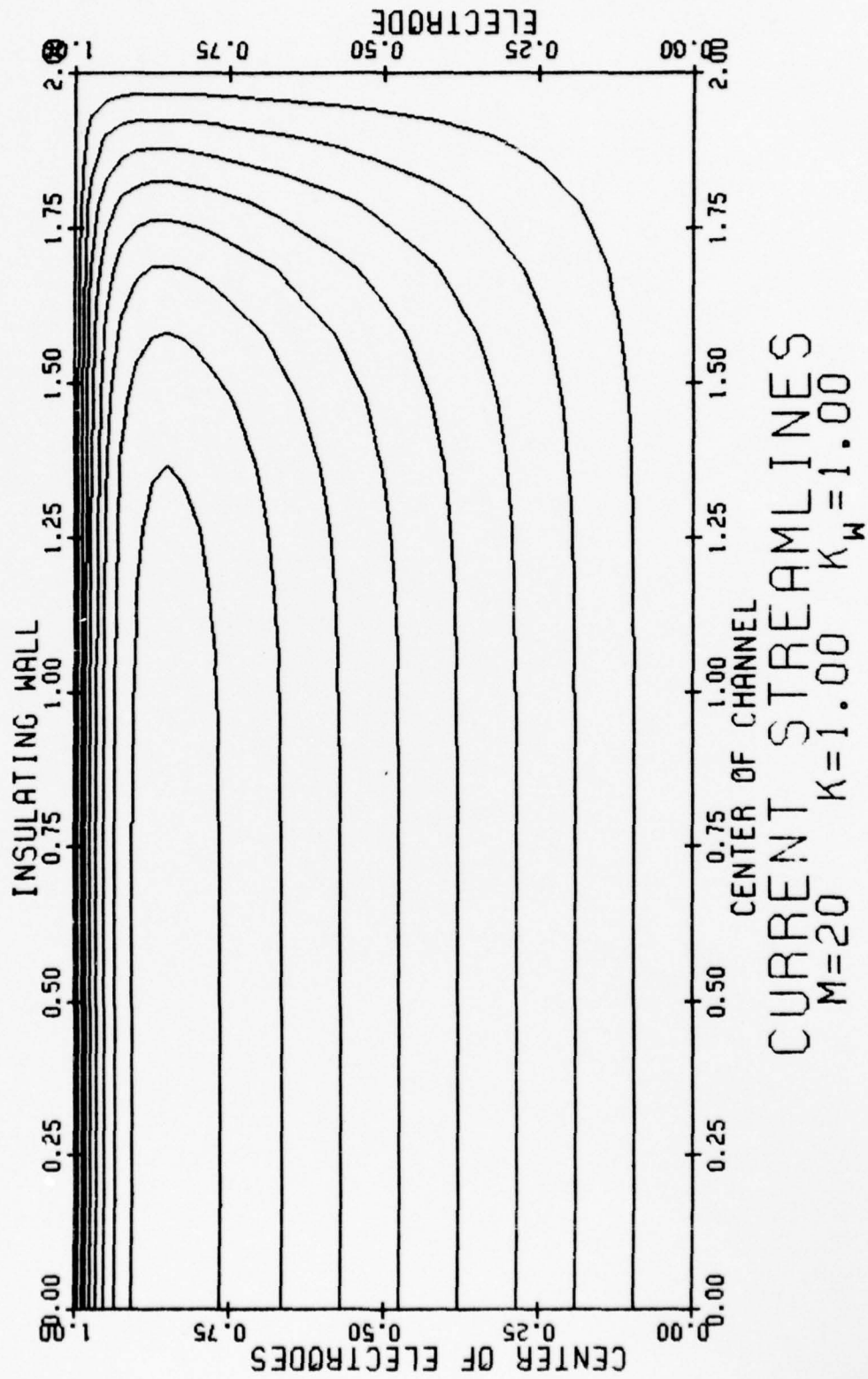


Fig. 7: Current Streamlines for Hartmann Flow with a Load Factor $K=1.0$ and Non-Conducting Electrodes ($K_W=1.0$).

the hyperbolic tangent profiles

$$\sigma = \sigma_0 / \{1 - (1/4)(1-A) [1 + \tanh 8(1-x/a)] [1 + \tanh 8(0.5-y/a)]\} , \quad (7)$$

where A is an adjustable parameter. Such a conductivity profile is an approximation to what can be expected in a two-phase MHD channel flow in which the conductivity near the wall is large but becomes quite small near the axis of the channel where most of the gas will be located. A calculation for A=10 is shown in Figs. 8 and 9. The load factor here is $K=0.95$ and the Hartmann number remains at $M=20$. Comparing these results with those obtained for constant electrical conductivity indicates the presence of a high velocity core near the channel axis followed by a velocity plateau at intermediate distances from the wall and then the usual rapid velocity decrease in the boundary layers. Note that this time there is a large current backflow in the vicinity of the insulating walls. This is the result mainly of the large load factor considered.

We have not at this point extended our calculations to larger Hartmann numbers in these two-dimensional calculations because of the increased computer time required. Ways to reduce the CPU time for larger M are now under investigation including the possibility of a boundary layer hookup with an inviscid core calculation. The calculation method could be used to make parametric studies with different viscosity and conductivity distributions should this seem advisable, and also used to determine volume flow rate as a function of channel aspect ratio. It is likely that the largest flow rates for a fixed area $4ab$ will occur in channels of aspect ratio $r=b/a$ less than unity as the boundary layers at the electrodes are generally thicker than the Hartmann layers at the insulating sides.

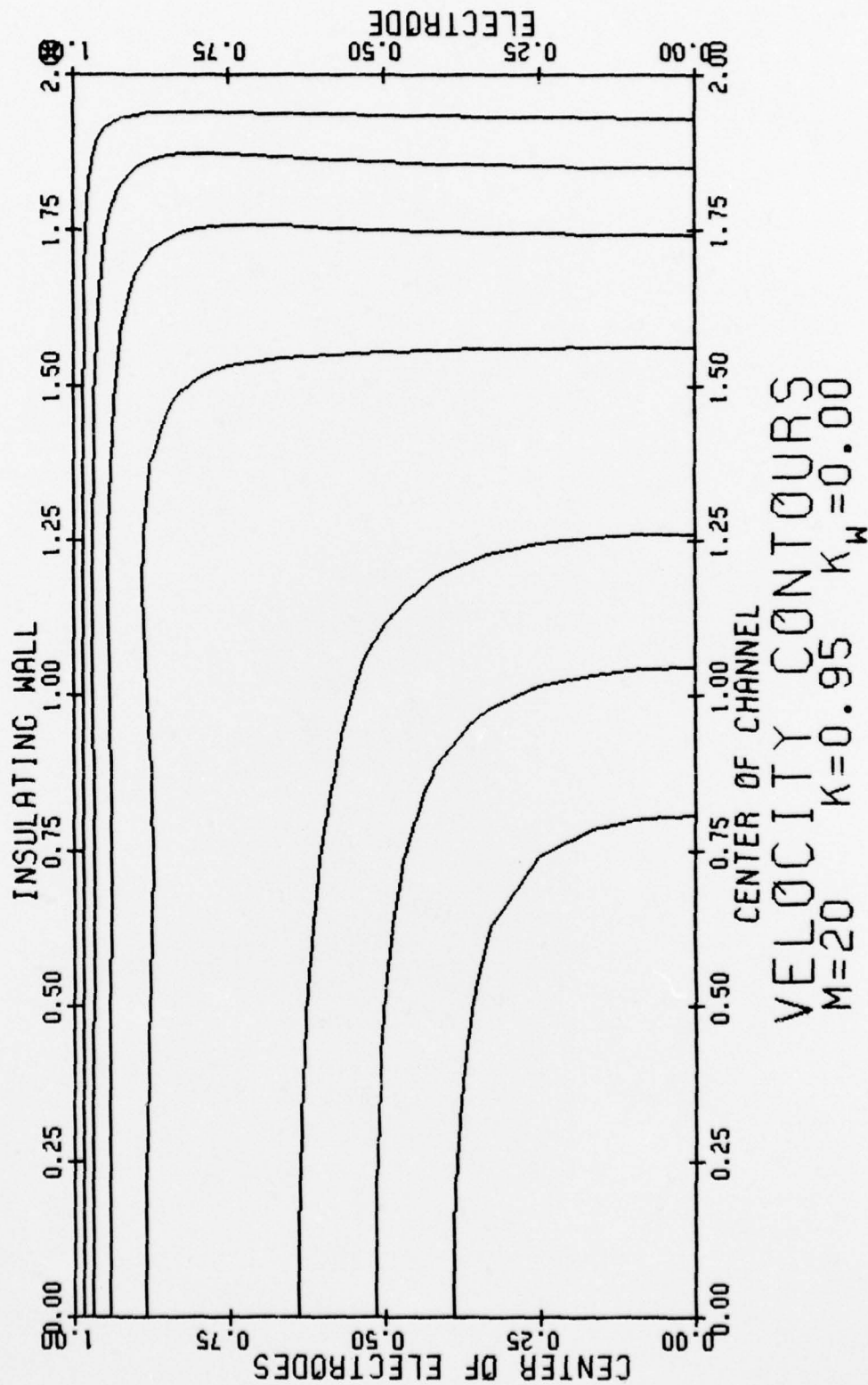


Fig. 8: Velocity Contours in MHD Channel Flow for the Variable Electrical Conductivity Distribution given by Eq. (7) with $A=10$. Hartmann Number $M=20$, Aspect Ratio $r=b/a=2$, Load Factor $K=0.95$ and Infinitely Conducting Electrodes ($K_w=0$).

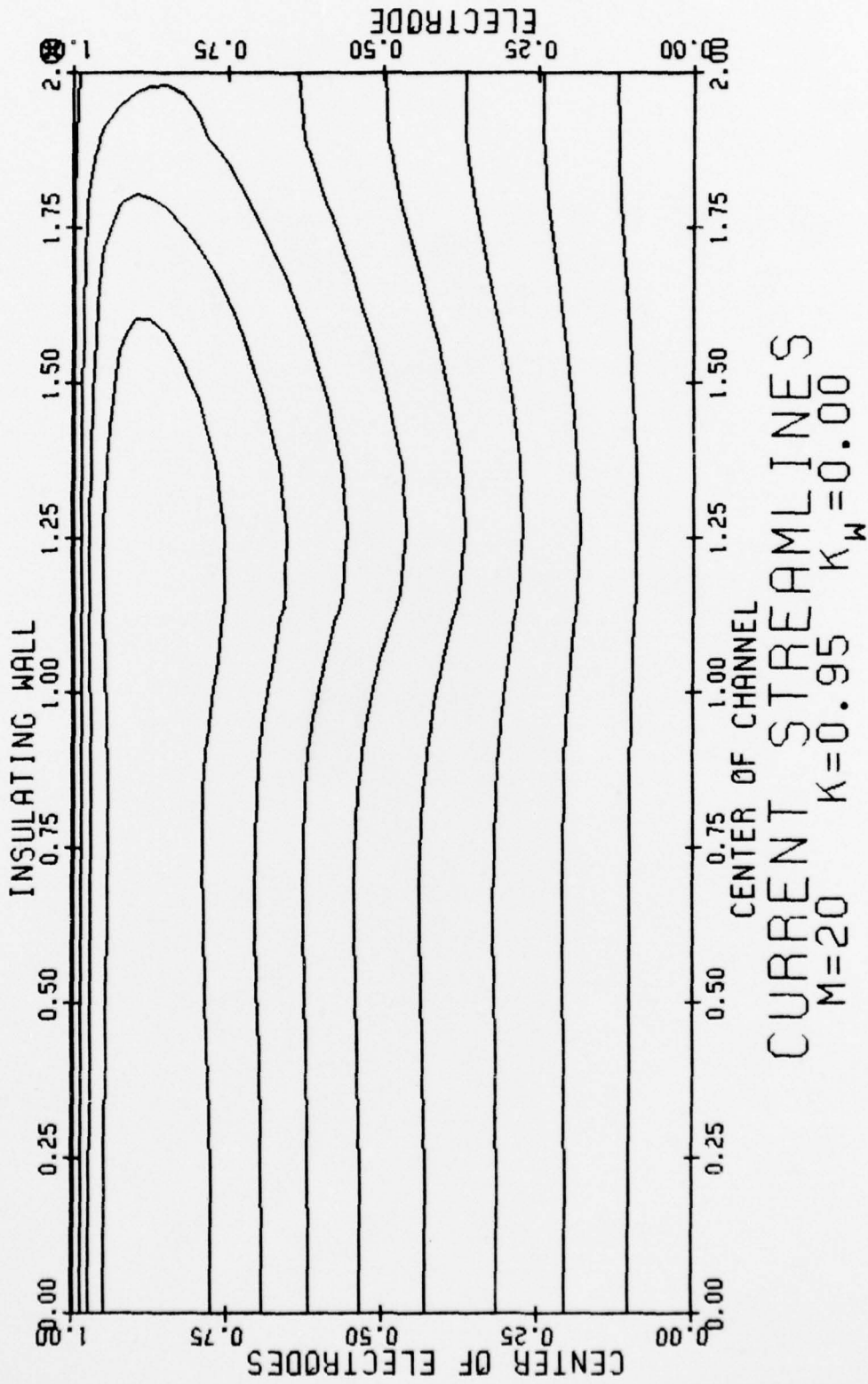


Fig. 9: Current Streamlines in MHD Channel Flow for the Variable Electrical Conductivity Distribution given by Eq. (7) with $A=10$.

IV. TWO-PHASE, ZERO-SLIP MODEL FOR COMPRESSIBLE MHD FLOW

In the two problems on Hartmann flow described above it has been assumed that there was no variation in conditions in the streamwise direction. This is generally not true in a two-phase MHD generator of the type under consideration at Argonne Laboratories where the gas in the two-phase flow undergoes considerable expansion between the entrance and exit part of the MHD channel. Accordingly, we have also devoted some time to examining existing one-dimensional two-phase slip models for which computer codes have been developed by the Argonne group [2] and attempted to develop some simplified version of their model which is consistent with the experimental observations and allows for time-variations in the variables. In particular, we examined the slip model used by them and feel that there are questions concerning the applicability of a churn turbulence term which is dependent on the presence of an average slip between the gas and liquid components. Measured variations in void fraction in the cross-stream direction could account for an apparent slip predicted by a one-dimensional approximation although locally there may be little velocity difference between the components. To have a reliance on such a one-dimensional model could lead to incorrect conclusions concerning the upscaling of two-phase MHD generators.

As a first approximation for the axial variations in the velocity, density, void fraction and pressure we have developed a one-dimensional isothermal, zero-slip model in which the gas is treated as ideal. Our objective is to use the zero-slip model, whose utility lies in its mathematical simplicity, to investigate the time-dependent behaviour of such flows and look for possible oscillatory phenomena that may be present and may lead to fluctuations in the power output in two-phase MHD generators. All flow properties in the cross-stream direction have been replaced by averages. Within the framework of these approximations, the governing time-dependent equations are essentially

those of bubbly two-phase flow as given by Wallis [9] after a magnetic force term is added. They become

$$\text{Continuity: } \frac{\partial \rho}{\partial t} + \frac{\partial}{\partial z}(\rho W) = 0 \quad (8)$$

$$\text{Momentum: } \rho \left(\frac{\partial W}{\partial t} + W \frac{\partial W}{\partial z} \right) = - \frac{\partial p}{\partial z} - \sigma B_o (E + WB_o) \quad (9)$$

$$\text{State(isothermal): } p = \text{const. } \rho_g \quad (10)$$

together with the subsidiary conditions

$$\text{Mean Density: } \rho = \alpha \rho_g + (1-\alpha) \rho_l \quad (11)$$

$$\text{Gas Continuity: } \frac{\partial}{\partial t}(\rho_g \alpha) + \frac{\partial}{\partial z}(\rho_g \alpha W) = 0 \quad (12)$$

Here all non-subscripted quantities refer to the averaged values at specified axial positions z . These equations have been solved by a finite difference-predictor-connector approach[8] using the conductivity void fraction relation given by eqs. (2) and (3). For one set of specified initial conditions and boundary conditions based upon constant pressure at the channel exit at $z = L$ and conservation of momentum, mass and energy during gas injection at the channel entrance at $z = 0$ and also closely approximating the conditions encountered in the low temperature NaK-N₂ MHD generator facility at Argonne Laboratories, one obtains the time-dependent velocity profiles shown in Fig. 10. For the large value of the interaction parameter $N = \sigma_o B_o^2 L / \rho W$ used in this calculation, the steady-state velocity condition is seen to be approached without any oscillatory behaviour. This was not always found to be the case at lower gas entrance pressures where transient oscillatory behaviour was sometimes observed. We are attempting at the moment to determine whether this oscillatory behaviour is due to numerical instabilities in the relaxation procedure used in the calculations or represents a real acoustic phenomenon which may produce the experimentally observed voltage fluctuations noted under

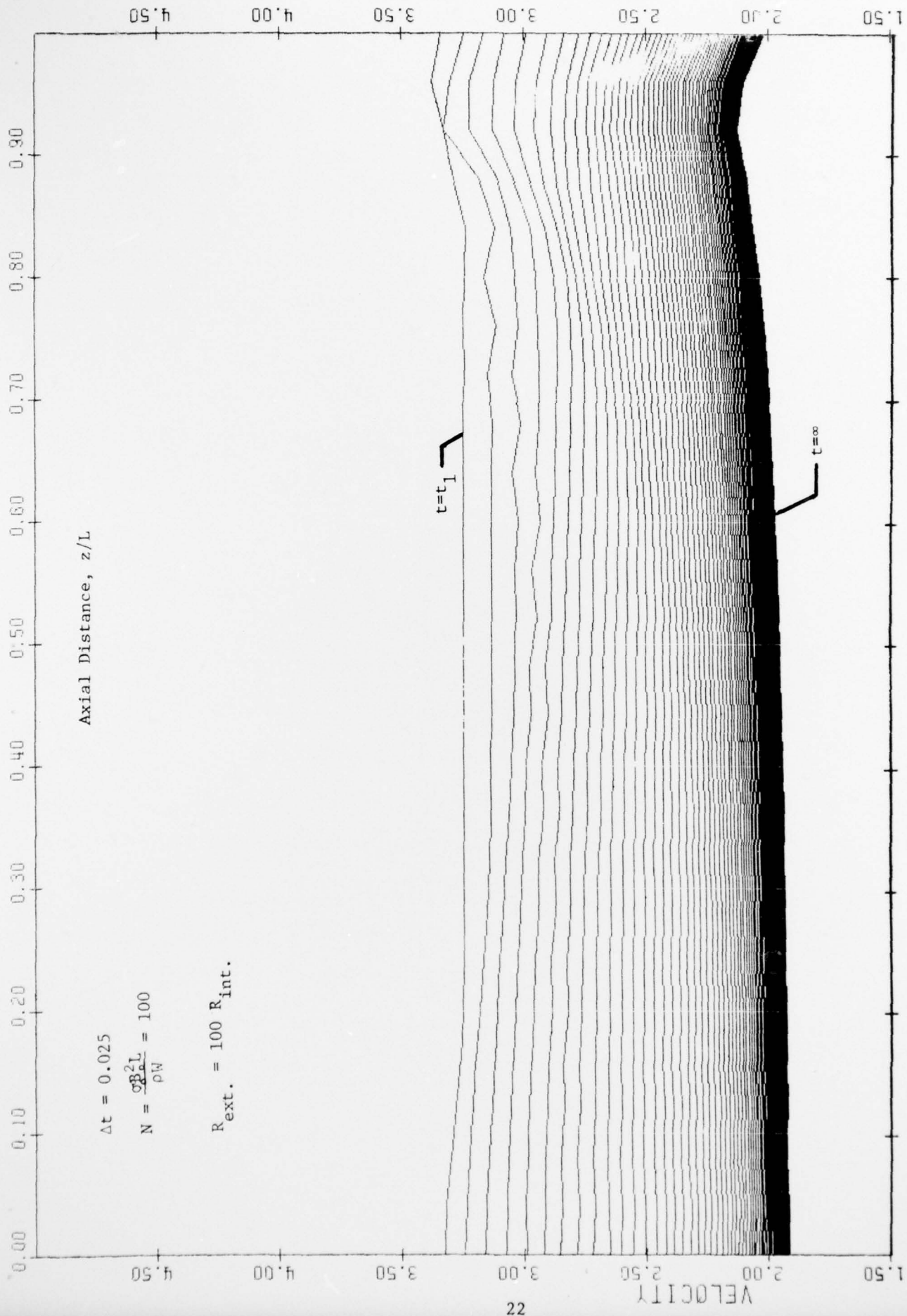


Fig.10: Time-Development of the One-Dimensional Velocity Distribution in the Two-Phase, Zero-Slip Model.

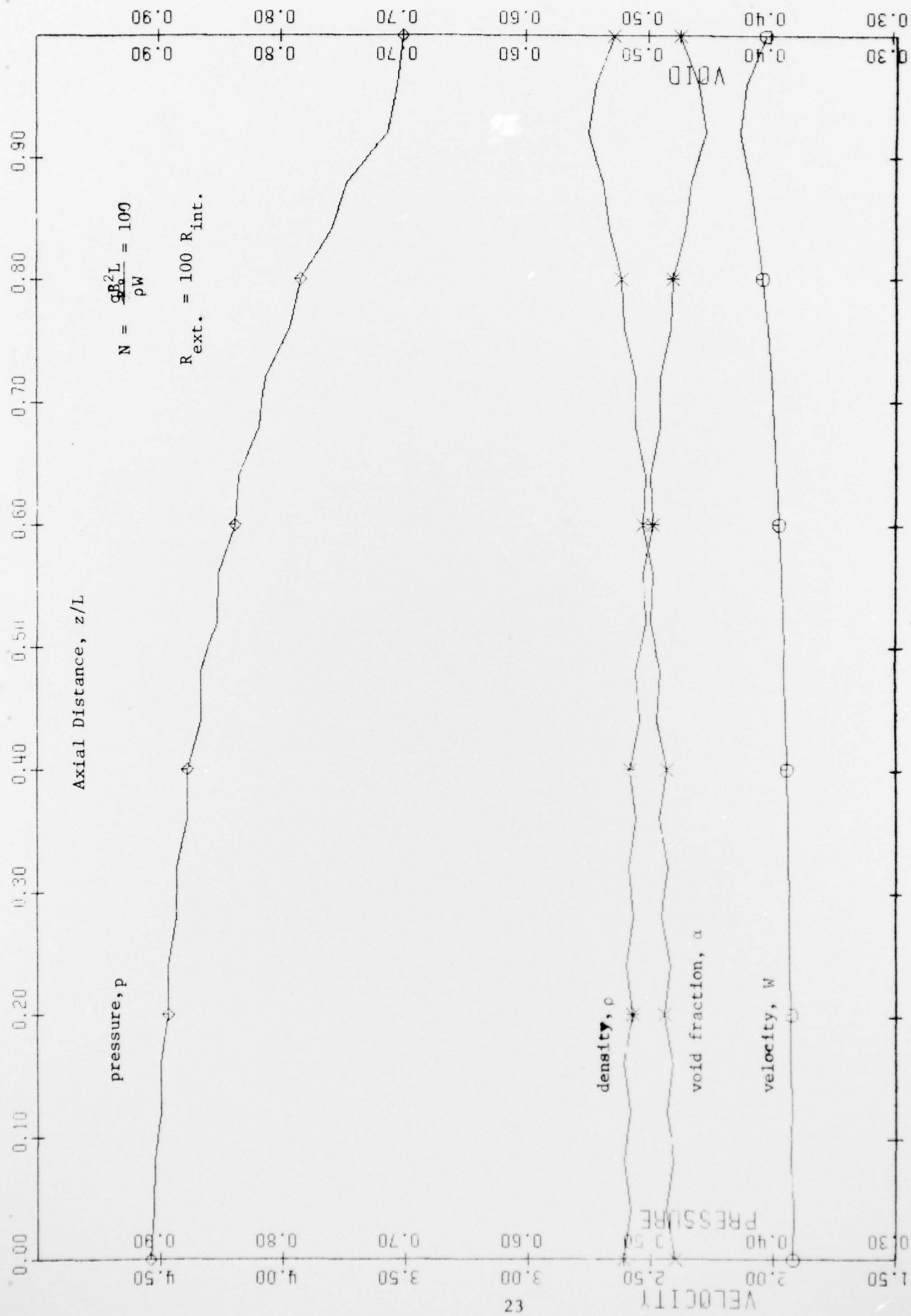


Fig.11: Steady-State Solution ($t \rightarrow \infty$) for the One-Dimensional, Zero-Slip, Two-Phase MHD Model.

certain conditions. In Fig. 11 we demonstrate the steady-state axially dependent pressure, density and void fraction corresponding to the steady-state velocity given in Fig. 10. Note, that as expected for the constant channel cross-section considered, the velocity and void fraction generally increase with increasing z while the pressure drops.

In connection with this zero-slip model we have also developed an approximate analytic model for channels of variable cross-section. This model, in which we neglect inertia forces and require the two-phase flow to remain sub-sonic, indicates that the velocity $W(z)$ generally increases with decreasing pressure and that approximate constant flow velocities desired in an MHD generator can be obtained by having an expanding channel and tailoring the local load factor by electrode segmentation. One of the shortcomings of the analytic model is that the acoustic velocity is not known a priori, being a function the gas pressure and the void fraction.

Some consideration has also been given to the expected sound velocity and concomitant potential compressible effects in the two-phase bubbly flows existing in liquid metal-gas MHD generators. Employing the standard approximation to the sound velocity in two-phase flows with void fractions in the range $0.1 < \alpha < 0.9$ as given in Ref. [9] and using the ideal gas law for assumed isothermal conditions we find that the sound velocity in the mixture becomes

$$c = \sqrt{\gamma p_g / [\alpha(1-\alpha)\rho_l]} \quad , \quad (13)$$

where γ is the specific heat ratio of the gas, p_g the gas pressure, ρ_l the liquid density and α the void fraction. The sound velocities predicted by this formula yield a minimum at $\alpha = 1/2$ and will take on values considerably lower than those existing in the fluid constituents taken separately. Typically, for a sodium-argon mixture at a channel gas pressure of 76 atmospheres, corresponding to the Argonne Laboratories high temperature facility [1], the sound

velocity will be 252 met./sec. This compares to an approximate minimum sonic velocity of 24 met./sec. in a water-air mixture at one atmosphere pressure. In view of formula (13) most of the existing experimental two-phase MHD generators operate under subsonic conditions. It may under certain circumstances be of advantage to operate such generators in a supersonic mode as this may help smooth out observed voltage fluctuations and produce an acoustically quieter flow.

V. CONCLUDING REMARKS

During the first year of our contract work on two-phase MHD flows we have treated the flows as essentially a homogeneous fluid with spatially dependent properties. This approach has yielded informative new results which probably will find direct application to some of the experimental work conducted in this area by M. Petrick of Argonne Laboratories and by H. Branover of Ben Gurion University. We have treated the flows as laminar. This can be partially justified by Branovers experimental studies[10] which indicate that turbulent fluctuations are essentially suppressed when the ratio of Hartmann number to Reynolds number exceeds a value of approximately 10^{-2} . It should be possible to meet this condition of turbulence suppression in experimental two-phase MHD generators.

We plan during the upcoming contract period to extend our investigations on two-dimensional Hartmann flows by making parametric studies of the volume flow rates through channels of rectangular cross-section for various different conductivity profiles. To handle the larger Hartmann number cases without the use of an inordinate amount of computer time, we will attempt to develop a boundary layer solution method in which the core of the flow is treated as inviscid. Also the effects of varying electrode conductivity and load factor will be further investigated.

The one-dimensional, compressible, no-slip model is to be examined further in order to determine the origin of the observed oscillations at lower entrance pressure conditions. We also intend to look at tapered channel geometries since it is desirable in actual two-phase MHD generators to keep the flow velocity constant in its passage through the generator duct. An

attempt will be made to include fluid property variations in the direction normal to the flow in order to account for the backflow currents existing in the Hartmann layers.

We have not up to the present time considered the dynamics of individual bubbles in these two phase flows, but plan to do so during the coming year because of the obvious importance of the suppression of radial bubble drift for a properly functioning generator. Analytical work on bubble drift in two-phase flows is nearly non-existent and presents a formidable problem. It might be that some type of flow separators will need to be installed in the two-phase flow channel to suppress such cross-stream bubble drifts.

Finally, some consideration will be given to the time development of Hartmann velocity profiles at the channel entrance. This problem is of great practical importance as the entrance lengths in typical MHD generators may be comparable with the actual channel length so that a steady-state profile may actually not exist.

REFERENCES

- [1] Petrick, M., Amend, W.E. et al "Investigation of Liquid Metal MHD Power Systems", Argonne National Laboratory Tech. Report ANL/ENG-72-06 (Dec. 1972).
- [2] Petrick, M., Amend, W.E. et al "Experimental Two-Phase Liquid Metal Magnetohydrodynamic Generator Program", Argonne National Laboratory Tech. Report ANL/ENG-73-02 (June 1973)
- [3] Hughes, W.F. and Young, F.J. The Electromagnetodynamics of Fluids, John Wiley and Sons, Inc. N.Y. (1966).
- [4] Shercliff, J.A. "Steady Motion of Conducting Fluids in Pipes under Transverse Magnetic Fields" Proc. Camb. Phil. Soc., 49, 136 (1953).
- [5] Uflyand, Y.S. "Flow Stability of a Conducting Fluid in a Rectangular Channel in a Transverse Magnetic Field" Soviet Tech. Phys. 5, 1191 (1960).
- [6] Chang, C.C. and Lundgren T.S. "Duct Flow in Magnetohydrodynamics" ZAMP, 12, 100 (1961).
- [7] Mitchell, A.R. Computational Methods in Partial Differential Equations, John Wiley and Sons, Inc., N.Y. (1976).
- [8] Hamming, R.W. Numerical Methods for Scientists and Engineers, McGraw Hill, N.Y. (1962).
- [9] Wallis, G.B. One-Dimensional Two-Phase Flow, McGraw Hill, Inc., N.Y. (1969).
- [10] Branover, H. and Gershon, P. "MHD Turbulence Study" Ben Gurion University Tech. Report RDA 100-76, Dept. of Mech. Eng. (April 1976).

REPORT DOCUMENTATION PAGE		READ INSTRUCTIONS BEFORE COMPLETING FORM
1. REPORT NUMBER 6	2. GOVT ACCESSION NO.	3. RECIPIENT'S CATALOG NUMBER
4. TITLE (and Subtitle) Two-Phase Hartmann Flows in the MHD Generator Configuration;		5. TYPE OF REPORT & PERIOD COVERED Annual Report, Dec. 75-Dec. 76
6. AUTHOR(s) E.R. Lindgren, U.H. Kurzweg, R.E. Elkins, and T.A. Trovillion		7. PERFORMING ORG. REPORT NUMBER
9. PERFORMING ORGANIZATION NAME AND ADDRESS Department of Engineering Sciences College of Engineering, University of Florida Gainesville, Florida 32611		8. CONTRACT OR GRANT NUMBER(s) N00014-76-C-0410 <i>New</i>
11. CONTROLLING OFFICE NAME AND ADDRESS Power Program, Material Sciences Division Office of Naval Research, 800 N. Quincy St. Arlington, Virginia 22217	10. PROGRAM ELEMENT, PROJECT, TASK AREA & WORK UNIT NUMBERS Task No. NR 099-412	12. REPORT DATE January 1977
14. MONITORING AGENCY NAME & ADDRESS (if different from Controlling Office) 12 35p.	13. NUMBER OF PAGES 28	15. SECURITY CLASS. (of this report) Unclassified
16. DISTRIBUTION STATEMENT (of this Report) Approved for public release; distribution unlimited		
17. DISTRIBUTION STATEMENT (of the abstract entered in Block 20, if different from Report)		
18. SUPPLEMENTARY NOTES		
19. KEY WORDS (Continue on reverse side if necessary and identify by block number) Magnetohydrodynamic Flows Two-Phase MHD Generators Hartmann Flows in Rectangular Channels		
20. ABSTRACT (Continue on reverse side if necessary and identify by block number) Two-phase Hartmann flows in an MHD generator duct of rectangular cross-section are examined and numerical values for the velocity fields and induced current streamlines for fluids of spatially-dependent electrical conductivity are determined as a function of load factor, Hartmann number and channel aspect ratio. This study is of considerable practical interest in connection with some experimental work in progress at Argonne Laboratories on two phase liquid metal-gas MHD generators and the results presented <i>→ next page</i> (continued on back)		

→ herein may enhance the understanding of the operating characteristics of such devices.) The problems considered include: 1) one-dimensional Hartmann flow between two parallel plates at high Hartmann number when the fluid electrical conductivity decreases with increasing distance from the walls, 2) two-dimensional Hartmann flow in rectangular channels of finite aspect ratio having two insulating walls and two thin walls of finite conductivity representing the electrodes and, 3) compressible one-dimensional isothermal MHD flow with zero-slip between its liquid and gas components. → Results indicate that conductivity gradients can produce inflected velocity profiles which may be hydrodynamically unstable, that for larger load factors the shunt current in the Hartmann boundary layers become considerable and that two-phase MHD flows of moderate void fractions have sound speeds considerably lower than in its components. Turbulent effects are not considered in these studies since turbulent fluctuations are expected to be suppressed for the high Hartmann number flows of interest in two-phase MHD generators.

Unclassified